Vu, T. T. A., Horsfield, B., Mahlstedt, N., Schenk, H. J., Kelemen, S. R., Walters, C. C., Kwiatek, P. J., Sykes, R. (2013): The structural evolution of organic matter during maturation of coals and its impact on petroleum potential and feedstock for the deep biosphere. - Organic Geochemistry, 62, 17-27

DOI: 10.1016/j.orggeochem.2013.06.011

THE STRUCTURAL EVOLUTION OF ORGANIC MATTER DURING MATURATION OF COALS AND ITS IMPACT ON PETROLEUM POTENTIAL AND FEEDSTOCK FOR THE DEEP BIOSPHERE

T. T. A. Vu [1,*], B. Horsfield[1], N. Mahlstedt[1], H.J., Schenk[2], S. R. Kelemen[3], C. C. Walters[3], P. J. Kwiatek[3], and R. Sykes[4]

1. Helmholtz Centre Potsdam, GFZ German Research Centre for Geosciences, Telegrafenberg, 14473 Potsdam, Germany

2. Forschungszentrum Jülich, Germany

3. ExxonMobil Research and Engineering Co., Annandale, NJ 08801

4. GNS Science, PO Box 30368, Lower Hutt 5040, New Zealand

[*] Corresponding author Tel.: +49(0)331 288-1976; Fax: +49(0)331 288-1782

E-mail: anhtiem@gfz-potsdam.de (T.T.A., Vu) or vu.anhtiem@gmail.com

Abstract

The structural evolution of coals during coalification from peat to the end of the high volatile bituminous coal rank (VR_r = 0.22−0.81%) has been studied using a natural maturity series from New Zealand. Samples were studied using a range of standard coal analyses, Rock-Eval analysis, infrared spectroscopy (IR), X-ray photoelectron spectroscopy (XPS), and pyrolysis gas chromatography (Py-GC). The structural evolution of coal during diagenesis and moderate catagenesis is dominated by defunctionalisation reactions leading to the release of significant amounts of oxygen and thereby to an enrichment of aromatic as well as aliphatic structures within the residual organic matter. Based on the evolution of pyrolysis yields and elemental compositions with maturity it can be demonstrated that oxygen loss is the major cause for increasing Hydrogen Index values or hydrocarbon generating potentials of coals at such maturity levels. For the first time, the loss of oxygen in form of CO_2 has been quantified. During maturation from peat to high volatile bituminous coal ranks ~10−105 mg CO_2/g TOC has been released. This is equivalent to 2.50E−4 to 1.25E−3 mg CO_2 generated from every litre of sediment per year falling into the range of deep biosphere utilisation rates. Immature coals, here New Zealand coals, therefore manifest the potential to feed deep terrestrial microbial life, in contrast to more mature coals (VR_r > ~0.81%) for which defunctionalisation processes become less important.

Key words: maturation, structural evolution, New Zealand coals, oxygen loss, elemental compositions, petroleum potential, feedstock, deep biosphere

1. Introduction

Humic coals are derived mainly from continental plants, contain identifiable vegetal debris, and are rich in humic macerals of the vitrinite group. On a molecular level, condensed aromatic and oxygen-containing structures are present in high abundance at immature maturation stages. As the organic matter in sediments is buried, its structure is no longer in equilibrium with its surroundings due to changes in both physical and chemical environment (Tissot and Welte, 1984). A large number of chemical reactions are involved in the thermal degradation of the organic matter. Many studies have been focused on the maturity range from shortly before beginning of the oil window to the end of oil expulsion to investigate the chemical changes affecting macromolecules (Marchand and Conard, 1980; Oberlin et al., 1980; Betrand, 1984; Witte et al., 1988; Levine, 1993; Landais, 1991; Requejo et al., 1992; Ibarra et al., 1996; Schenk and Horsfield, 1998; Sykes and Snowdow, 2002). However, relatively little attention has been directed to the structural evolution of organic matter during diagenesis (Kelemen et al., 2002, 2007; Salmon et al., 2009).

During maturation, the organic matter within coals is subjected to both cracking and aromatization/condensation mechanisms (Stach et al., 1982; Tissot and Welte, 1984; Solomon, 1988; Schenk and Horsfield, 1998; Taylor et al., 1998), which causes a progressive elimination of functional groups and linkages between nuclei, an increase in the average stacking number of aromatic sheets, and a more condensed solid residue (Requejo et al., 1992, Ibarra et al., 1996, Kelemen et al., 2007). Loss of oxygen during maturation of coals is well known and detectable by a decrease of atomic O/C ratios, a decrease in related absolute oxygen contents (wt.%) and infrared –OH, −COOH, C=O adsorption intensities, as well as an increase of water and CO/CO_2 production (Tissot et al.,

60 1974; Robin and Rouxhet, 1978; Durand and Monin, 1980; Boudou et al., 1984; Behar et
61 al., 1995; Charpenay et al., 1996; Ibarra et al., 1996; Kelemen et al., 2002). Consequently,
62 coals release a high amount of oxygenated compounds (CO_2, H_2O, and organic acids),
63 hydrogen and hydrocarbons (Tissot and Welte, 1984; Carr and Williamson, 1990; Payne
64 and Ortoleva, 2001). These compounds can act as a substrate for the deep biosphere (Rice
65 and Claypool, 1981; Parkes et al., 2000; Horsfield et al., 2006), which has been detected as
66 deep as 1km below the seafloor or 3km below continental surfaces (Horsfield and Kieft,
67 2007; Fang and Zhang, 2011). Living at such depth, microbes are fully detached from
68 surface processes, its energy and food supplies. It is suggested that organic-rich lithologies
69 represent potential feeders, whereas others, such as coarse-grained sandstones, are
70 potential hosts to microbial ecosystems (L´Haridon et al., 1995; Krumholz et al., 1997;
71 Horsfield et al., 2006). Low rank coals appear to be essentially well suited for feeding the
72 deep subsurface microbes (Horsfield et al., 2006; Vieth et al. 2008; Glombitza et al. 2009a,
73 2009b, 2011). The question remains whether the approximate amount of oxygen released
74 during maturation of coal can be quantified, thereby providing a bulk quantitative feeding
75 potential for the deep biosphere (e.g., methanogens)?

76 The New Zealand Coal Band was chosen because it provides an essentially
77 continuous series of coal ranks from peat through high volatile bituminous coals with very
78 little facies variation and a consistent richness in vitrinite (Killops et al., 1994; 1998;
79 Newman, 1997; Norgate et al., 1997; Suggate, 2000; Sykes, 2004; Sykes et al., 2004; Vu et
80 al., 2008; 2009). The New Zealand coals are characterised by increasing Hydrogen Index
81 values (HI = S2×100/TOC) during early diagenesis to moderate catagenesis (Suggate and
82 Boudou, 1993; Killops et al., 1998; Sykes and Snowdon, 2002; Vu, 2008; Vu et al., 2008).
83 This feature is also reported for many immature coals from other parts of the world
84 (Durand and Paratte, 1983; Marquis et al., 1992; Boreham et al., 1999), which is in

contrast to the common understanding that HI values of mature coals as well as of other mature kerogen types strongly decrease with maturation (Espitalié et al., 1985; Hetényi and Sajgó, 1990; Requejo et al., 1992; Sykes and Snowdow, 2002; Jasper et al., 2009). Two main concepts, explaining the increase in HI during diagenesis, have been put forward. The first one, a concentration concept, claims that the release of large amounts of CO_2, CO and other functionalised groups at low levels of maturity lead to an enrichment of potential hydrocarbon generating structures (Durand and Paratte, 1983; Vandenbroucke and Largeau, 2007). The second concept assumes that the increase in the petroleum generating potential of coals is rather caused by a structural rearrangement of the macromolecular matrix, which results in the formation of significant amounts of new bonds with different generation potentials (Killops et al., 1998; Schenk and Horsfield, 1998; Sykes and Snowdon, 2002). Killops et al. (1996; 1998) pointed out using mass balance calculations that simple loss of CO_2 could only account for an increase in HI of roughly 10 mg/g TOC, which would be less than 10% of the HI increase (up to 150 mg/g TOC) observed for New Zealand coals. Nevertheless, coals from the New Zealand Coal Band show no appreciable increase in atomic H/C ratios over the maturity range VR_r = ~0.35% – ~0.80% (Sykes and Snowdon, 2002; Vu, 2008).

In this paper, we aim firstly to investigate the structural changes of organic matter in coal during diagenesis to early catagenesis. Secondly, this paper revisits the importance of oxygen loss for the HI increase prior to catagenesis (VR_r = 0.81%). Thirdly, we attempt to calculate the loss of oxygen released as CO_2 from the decrease of Oxygen Index (OI = S3×100/TOC) values during maturation thereby providing a bulk quantitative feeding potential for the deep biosphere.

2. Material and methods

A set of immature Late Cretaceous-Tertiary New Zealand coals samples (VR_r = 0.22% − 0.81%) was available for studying the structural evolution of organic matter during maturation using infrared spectrometry, Rock-Eval pyrolysis and pyrolysis-gas chromatography (Table 1). X-ray photoelectron spectroscopy (XPS) data of immature New Zealand coals was compared to XPS data published in Kelement et al. (2002) for a maturity equivalent coal sample set (Argonne Premium (AP) Coal Sample Program, and DECS and PSOC coals selected from the Pennsylvania State University coal sample bank). This helps to complete the picture of organic macromolecular structure evolution during coalification and to observe the alterations of pyrolysate compositions as a function of rank.

A range of standard coal analyses was performed on milled New Zealand sub-samples by CRL Energy Ltd., New Zealand, following international and in-house standard procedures. These analyses included proximate analysis [moisture (M), ash (A) and volatile matter (VM)], ultimate analysis [C, H, N, S, O; dry and ash free (daf) basic], and calorific value (CV; specific energy). Adjustments of CV and VM to the dry, mineral matter and sulfur free (dmmsf) basis and atomic O/C and H/C to the mineral matter free (mmf) basis, for determination of Rank(S_r) values, were made using the formulas of Suggate (2000). Rank(S_r) was designed to accommodate variation in coal kerogen type through the use of two parameters, VM and CV or atomic H/C and O/C (Suggate, 1959, 2000, 2002; Sykes et al., 1992). The investigated sample set (Group A and B) was carefully selected from the New Zealand Coal Band based on the VM vs. CV diagram for intensive studies on the changes of organic matter properties during early stages of maturation. As illustrated in Fig. 1, this sample set (especially the Group A) is a very homogenous maturation sequence, with very minor facies variations. These samples have

134 also been studied in previous publications (Vieth et al., 2008; Vu et al., 2008, 2009;
135 Glombitza et al., 2009a, 2009b, 2011; Mahlstedt and Horsfield, 2012). Details on
136 geological age, origin, maturity level, organic matter type, and depositional environment
137 are given in these publications.

138 Vitrinite reflectance was measured by Newman Energy Research Ltd., New
139 Zealand, on polished grain mounts using a Zeiss MPM 400 petrological microscope.
140 Measurements of VR_r (random) were made on 50 telovitrinite or telohuminite subjects in
141 each sample. Although quantitative maceral group determinations have not been
142 undertaken, observations of petrographic composition during the course of the vitrinite
143 reflectance analyses showed that all samples are heavily dominated by vitrinite, and none
144 of them is particularly rich in inertinite or liptinite. This is supported by the fact that at
145 least all group A samples plot in the middle of the New Zealand Coal Band on the VM vs
146 CV diagram (Fig. 1).

147 For organic geochemical analyses, New Zealand samples were freeze dried (48 h)
148 and ground to <200 mesh in a disc mill (15 s), then stored under nitrogen. Total organic
149 carbon (TOC) contents were determined using a LECO^{TM}-CNS-2000 elemental analyser.
150 The Rock-Eval parameters were determined using a Rock-Eval 6 instrument. Ten of the
151 twenty-three samples (Group A) and six samples of Group B were selected for infrared
152 spectroscopy, which were recorded on a Perkin-Elmer 783 dispersive spectrophotometer
153 coupled to a Spectrafile IR plus-2.00 data station at ForschungsZentrum Jülich Germany.
154 KBr pellets with varying amounts of coal (1–2 mg) were prepared according to the
155 published procedures in Schenk et al. (1986). The integrated infrared absorptions (cm/mg
156 TOC) in selected spectral ranges of selected New Zealand coals are given in Table 2.

157 The same sixteen samples were further analysed using XPS, a surface sensitive
158 technique (Kelemen and Kwiatek, 1995; Kelemen et al., 2002; 2007), which enables the
159 direct quantification of oxygen and its functionalities as well as other elements (e.g. total
160 aromatic carbon, sulphur and nitrogen). Samples were prepared according to the
161 procedures published in Kelemen and Kwiatek (1995) and Kelemen et al. (2002; 2007).
162 The relative amount of aromatic carbon was determined by the method Π and Π^* of signal
163 intensity (Kelemen et al., 1993). The amount of organic oxygen was derived from the total
164 oxygen (1s) signal by taking into account inorganic contributions. Organic oxygen forms
165 were determined by analysing the effect of oxygen on the XPS carbon (1s) signal of
166 adjacent carbon atoms. Five peaks were used to curve-resolve the XPS carbon (1s) signal.
167 These occur at 284.8, 285.3, 286.3, 287.5, and 289.0 (±0.1) eV. The 284.8 eV peak
168 represents contributions from both aromatic and aliphatic carbon. The 286.3 eV peak
169 represents carbon bound to one oxygen by a single bond (e.g., C−O, C−OH, etc.). The
170 287.5 eV peak corresponds to carbon bound to oxygen by two oxygen bonds (C=O and
171 O−C−O). The 289.0 eV peak corresponds mainly to carbon bound to oxygen by three
172 bonds (O=C−O). The 285.3 peak will have contributions mainly from carbon adjacent to
173 carboxyl carbon (beta peak) and carbon bound to nitrogen (i.e., pyrrole and pyridinic). The
174 285.3 eV peak is therefore fixed to the sum of the intensity of the 289.0 eV peak and the
175 intensity of carbon adjacent to nitrogen (i.e., twice the nitrogen level). The XPS data are
176 shown in Table 3.

177 Pyrolysis gas chromatography was performed using the Quantum MSSV-2 Thermal
178 Analysis System© for New Zealand coal samples in Group A. The thermally extracted
179 (300°C for 10 minutes) sample was heated in a flow of helium, and products released over
180 the temperature range 300-600°C (40K/min) were focussed using a cryogenic trap, and
181 then analysed using a 50m x 0.32mm BP-1 capillary column equipped with a flame

ionisation detector. The GC oven temperature was programmed from 40°C to 320°C at 8°C/minute. Boiling ranges (C_1, C_2−C_5, C_6−C_{14} and C_{15+}) and individual compounds (*n*-alkenes, *n*-alkanes, alkylaromatic hydrocarbons) were quantified by external standardisation using *n*-butane. Response factors for all compounds were assumed the same, except for methane whose response factor was 1.1.

3. Results and discussion

3.1. Structural evolution of organic matter in coals from early diagenesis to moderate catagenesis

All geochemical parameters obtained from spectroscopic (IR, XPS) and pyrolytic investigations reflect a systematic change of the coal structure as a function of vitrinite reflectance, i.e. maturity level (Figs. 2−5). Significant loss of oxygen in the evolution interval 0.22−0.81% VR_r is the major characteristic of diagenesis to moderate catagenesis (Figs. 2−3). A direct consequence of oxygen loss, as will be demonstrated later on in detail, is an increase in hydrocarbon generating potentials from 120 to ~260 mg HC/g TOC at VR_r ~0.80% (Fig. 4), a feature confirmed by increasing pyrolysis production yields (Fig. 5e). Natural maturation of coals at this maturity stage is further characterized by an enrichment of aromatic structures (Figs. 5b, 5d) as well as by only a slight increase in the amount of aliphatic structures with concomitant enrichment of methylene over methyl functionalities (Fig. 5c). The decrease of ali-C observable in Figure 5d is related to normalisation of aromatic and aliphatic carbon to 100 C atoms, and indicates not a loss in aliphatic carbon but a relative gain in aromatic carbon due to not only concentration but additionally “neoformation” in the course of carbon bound oxygen loss. Similar absolute aliphatic carbon contents on a cm/g TOC basis (Fig. 5c) are not in direct contrast to current models of coal maturation, which rather assume a depletion of aliphatic structures in the

residual coal as a consequence of hydrocarbon generation (Requejo et al., 1992; Ibarra et al., 1996; Kelemen et al., 2002; 2007), but demonstrates the importance to treat such models with caution at low maturity ranges. In line with those considerations, Al Sandouk et al. (2013) also report that aliphatic moieties in bulk kerogen concentrates increase with maturation (VR_r = 0.45–0.68%).

The loss of oxygen during maturation from 0.22% to 0.81% VR_r is directly revealed by a significant and log-linear decrease of O/C atomic ratios from 0.343 to 0.068 (Fig. 2a), a continuous decrease of absolute oxygen contents from ~30 wt.% to 10 wt.% (Fig. 2b), a linear decrease of moisture contents from 30% to 3% (Fig. 2c), by a strong decrease of Rock-Eval OI values from 100 mg CO_2/g TOC to 5 mg CO_2/g TOC (Fig. 2d) and by a decrease of total organic oxygen from around 25 to 7 (amount per 100C) (Fig. 2e). The relevant maturity range corresponds to the first (immature) maturation stage described in Durand and Monin (1980), where oxygen defunctionalisation reactions prevail and especially C=O functionalities (IR) rapidly disappear (also compare Fig. 2f), resulting in the formation of CO_2, H_2O and heavy heteroatomic products, e.g., resins, asphaltenes. A direct quantification of different oxygen functional groups (XPS) within immature New Zealand coal reveals, in comparison to XPS-data obtained by Kelemen et al. (2002) for a series of immature to highly mature coals (VR_r = 0.23–5.45%) (Fig. 3), that earlier findings are still valid and in agreement with data published in Kelemen et al. (2002). A preferential loss of oxygen fixed in relatively volatile functional groups (e.g., carboxylic acids, ester) rather than of oxygen fixed in stable groups (e.g., phenolic −OH group, ethers) is indicated. As shown in Fig. 5f, pyrolysis yields of phenolic compounds are almost unchanged during diagenesis and rather slightly increase up to 0.80% VR_r. Even though amounts of oxygen in both C−O single bond species (Fig. 3a) and carboxyl groups (O−C=O) (Fig. 3b) decrease from VR_r = 0.22% to VR_r = 0.81%, their relative proportions change, with

231 O−C=O decreasing from ~40% to ~0% and C−O single bounded species increasing from
232 ~42% to ~100% (Fig. 3d). The amount of oxygen in carbonyl groups (C=O) also generally
233 decreases (Fig. 3c), with relative proportions varying between ~25% and ~5% (Fig. 3d).

234 A second important feature of coalification from 0.22% to 0.81% VR_r is that HI
235 values of investigated New Zealand coals strongly increase from 124 to ~260 mg HC/g
236 TOC) with increasing maturity level (Figs. 4a, 5a), whereas H/C atomic ratios rather
237 decrease or scatter within a narrow range of 0.901–0.778 (Figs. 2a, 4c). The relationship
238 between elemental compositions and Rock-Eval parameters as expressed by Espitalié et al.
239 (1977) stating that there is a good correlation between HI and H/C ratio, as well as OI and
240 O/C ratio, is therefore too simple, which is best seen in Fig. 4c illustrating a very poor fit
241 between H/C and measured HI values ($R^2 = 0.14$). Interestingly, hydrocarbon generating
242 potential does not increase with increasing atomic H/C ratios, but rather increases with
243 atomic O/C ratios decreasing from 0.343 to 0.068 (correlation $R^2 = 0.84$) (Fig. 4d). Orr
244 (1981) also examined the relation between elemental compositions and pyrolytic
245 hydrocarbon yields, using a sample set exhibiting a broad range of atomic H/C (0.71- 1.55)
246 and a more restricted O/C (0.08- 0.19) ratio range. The author provided an equation
247 describing a systematic relation between elemental compositions and pyrolytic
248 hydrocarbon yields, which can be expressed as

249 $$HI = 694 \times (H/C - 0.29) - 800 \times (O/C)$$ (*Equation 1*).

250 Applying this equation to the investigated New Zealand coal series (Group A), a very good
251 fit (linear regression $y = 0.93 \times x$ with $R^2 = 0.92$) between calculated HI values and directly
252 measured HI values is attained (Fig. 4b). It can be concluded that there is a systematic
253 correlation between elemental compositions (H/C, O/C) and measured HI values from
254 Rock-Eval analysis and that the evolution of HI during diagenesis to moderate catagenesis

255 is strongly related to changes in O/C atomic ratios rather than to changes in H/C atomic
256 ratios. In other words, it can be deduced that the loss of oxygen containing molecules is the
257 major cause for the increase in HI values up to VR_r ~0.80% by concentration of potential
258 hydrocarbon generating structures (Durand and Paratte, 1983; Vandenbroucke and
259 Largeau, 2007), and that here rearrangement of the coal structure (Schenk and Horsfield,
260 1998) as suggested by Killops et al. (1998) and Sykes and Snowdon (2002) plays only a
261 minor role. Furthermore, a postulated rearrangement of organic matter structures involving
262 incorporation of hydrogen-rich volatile components into the coal matrix would result in a
263 higher oil-proneness of mature coals compared to immature ones (Boreham et a., 1999;
264 Sykes and Snowdon, 2002), and should thus cause a marked decrease in gas-oil-ratio
265 (GOR) values. However, our data show relative constant pyrolysis GOR (Fig. 5h) and gas
266 wetness values (Tab. 1) for New Zealand coals during diagenesis and moderate catagenesis
267 rather hinting to the relevance of the concentration concept.

268 Concentration of potential hydrocarbon generating structures within the coals
269 organic matter by defunctionalisation of oxygen containing structures leads not only to an
270 increase in the hydrocarbon generating potential (Fig. 5a) but consequently also to a
271 relative enrichment of protonated aromatic carbon (Fig. 5b) and total aliphatic carbon (Fig.
272 5c). Nevertheless, some structural changes and "rearrangements" do occur, which can be
273 deduced from a decrease in the $CH_3/(CH_3+CH_2)$ ratio (Fig. 5c), from a relative increase of
274 aromatic carbon on the costs of aliphatic carbon (Fig. 5d), and from differences in the
275 evolution of single compounds and boiling fractions pyrolysis yields (Figs. 5e−h).

276 The decrease in the $CH_3/(CH_3+CH_2)$ ratio (Fig. 5c) is related to the loss of methyl
277 groups together with the most unstable oxygen bearing functional groups rather than to an
278 absolute increase in methylene functionalities and thus aliphatic carbon chain length. A
279 general decrease in the average aliphatic carbon chain length over a comparable maturity

range (VR_r = 0.35−1.20%, calculated from T_{max} values) was demonstrated for different coals and kerogen types in various studies using NMR (Requejo et al., 1992; Kelemen et al., 2002; 2007). In addition, based on alkaline ester cleavage experiments, Glombitza et al. (2009b) reported for the here used New Zealand coals sample set that concentrations of liberated low molecular weight compounds such as acetate, which possess a methyl group within its chemical structure, considerably decrease during early diagenesis up to maturity levels of about 0.6% VR_r indicating a continuous loss of kerogen-linked small organic acids during maturation of organic matter, whether by release from or incorporation into the residual kerogen.

The increase in amount of total aromatic carbon per 100 C from ~40 to ~70 with maturity increasing from 0.22% VR_r to 0.81% VR_r for the New Zealand coals is, regardless of different geological regions, similar to the increase observed by Kelemen et al. (2002) for another coal sample set (Fig. 5d). It is also the strongest indication that, besides simple concentration of hydrocarbon generating structures, structural changes such as aromatisation of e.g. alicyclic ring components (Schenk and Richter, 1995) or condensation take place, as the proportion of aliphatic carbon per 100 C (Fig. 5d) mathematically decreases from maximal 40 at VR_r = 0.22% to 12 at VR_r = 0.81%. Interestingly and as mentioned before, HI values increase and so do pyrolysis gas and C_{6+} yields, which leads to constant GOR values (Figs. 5a, 5e and 5h respectively). However, considering generated amounts of single compounds, yields of aliphatic *n*-C_{6+} compounds increase (Fig. 5f) whereas yields of aromatic compounds such as phenols, monoaromatics or diaromatics, stay roughly constant or only slightly increase (Figs. 5f−g) leading to a slight decrease in the aromaticity (Tab. 1), defined as aromatic moieties divided by *n*-alkyl moieties in the C_{6+} pyrolysis products. It can be therefore deduced that the net increase in total aromatic carbon (Fig. 5d) is also related to an incorporation of aromatic precursor

structures into a refractory/dead or at least GC-unamenable moiety of residual organic matter.

3.2. Feedstock for the deep biosphere

It is known that terrigenous organic matter, especially coals, can generate high amounts of low molecular weight oxygenated compounds (e.g., CO_2, organic acids) and probably hydrogen (via aromatisation reactions) during diagenesis and catagenesis (Tissot et al., 1974; Durand and Monin, 1980; Carr and Williamson, 1990; Payne and Ortoleva, 2001). These compounds can be sustained in ecosystems that are fully detached from surfaces processes (Rice and Claypool, 1981; Parkes et al., 2000; Horsfield et al., 2006). Here, we aim to measure or calculate the quantitative feedstock potential of terrestrial organic matter for deep biosphere ecosystems. Therefore, the loss of oxygen as CO_2 has been quantified based on the evolution of OI with maturation. This quantification is formulated in the same way in which yields of hydrocarbons were quantified by Pelet (1985). In general, the Transformation Ratio of kerogen to hydrocarbon conversion (TR_{HC}) is calculated from the decrease of HI observed for the progressive maturation of any given source rock maturity series. Similarly, there is a significant decrease in OI values during diagenesis and moderate catagenesis, which has been discussed in Section 3.1. Therefore and with these considerations in mind, a new Transformation Ratio for kerogen to CO_2 conversion (TR_{CO2}) has been expressed (*Equation 2*) in order to quantify the loss of oxygen as CO_2:

$$TR_{CO_2} = \left[\frac{3600 \times \left(OI_0 - OI_x \right)}{OI_0 \times \left(3600 - OI_x \right)} \right] \qquad \text{(Equation 2)}$$

where OI_0 = Oxygen Index of immature sample

OI_x = Oxygen Index of mature sample

3600 represents the reciprocal (times 1000) of the carbon proportion in CO_2

The TR_{CO2} is plotted versus vitrinite reflectance in Fig. 6a, calculated values are given in Tab. 4. One can see at first sight that values do follow a rank-related trend. The TR_{CO2} increases as a function of maturity and reaches 95% of conversion at VR_r = 0.70%. In order to calculate the amount of released oxygen during maturation, oxygen yields were renormalized to the original organic content of the original sample using *Equation 3*:

$$OI_i = \left[\frac{OI_x \times (3600 - OI_0)}{(3600 - OI_x)} \right] \quad \text{(Equation 3)}$$

Where: OI_i = Oxygen Index of mature sample normalised to original TOC

OI_0 = Oxygen Index of immature sample

OI_x = Oxygen Index of mature sample

3600 represents the reciprocal (times 1000) of the carbon proportion in CO_2

Oxygen yields are expressed in CO_2 and illustrated in Fig. 6b as a function of TR_{CO2}. Yields range from 10 to 104 mg CO_2/g TOC during maturation from peat to high volatile bituminous coal ranks. This is equivalent to 0.23 to 2.4 millimoles CO_2 per gram of organic carbon. As an aside, e.g. for methanogenesis via CO_2 reduction, four moles of hydrogen would be required. Thus, between 0.92 and 9.6 millimoles hydrogen would be required for complete CO_2 reduction.

Considering the feeding potential of the investigated New Zealand coals for deep microbial life, the released CO_2 amounts are compared to CO_2 respiration rates (4.40E−5

to 4.40E−2 mg per litre per year) reported for deep-aquifer systems (Tab. 5) by D´Hondt et al. (2002). The estimated yield of CO_2 released from immature samples within the Pleistocene over a time span of 2 Ma is 10 mg/g TOC, whilst the estimated yield of CO_2 released from now mature New Zealand coal samples since the Late Cretaceous (~100 Ma) is as high as 100 mg/g TOC. Considering the case of the least mature sample (i.e. the starting point) with TOC contents of ~50%, and assuming a sediment density of 2 kg/l, approximately 2.50E−4 to 1.25E−3 mg CO_2 would be generated from every litre of sediment per year for coals of peat to the end of high volatile bituminous coal rank and from Late Cretaceous to Pleistocene geological ages. This rate falls into the range of deep biosphere utilisation rates (Tab. 5). Therefore, it is concluded that during maturation, especially during early diagenesis to moderate catagenesis, the thermal alteration of organic matter in coals leads to the release of sufficient feedstock to sustain deep microbial life (e.g. methanogens).

Additionally and almost completely overlooked is the fact that low rank coals exhibit high extraction yield of up to 200 mg/g TOC (Durand et al., 1977; Hvoslef et al., 1988; Bechtel et al., 2005; Avramidis and Zelilidis, 2007; Vu et al., 2009). The water-soluble low molecular weight organic acids (LMWOAs), such as formic acid, acetic acid and oxalic acid, are considered as a potential carbon source to feed the deep biosphere (Vieth et al., 2008). Glombitza et al. (2009b) report an obvious depletion of LMWOAs released by alkaline ester cleavage as a function of maturity using the here described New Zealand coal series. Formate, acetate and oxalate were detected in significant amounts and found to rapidly decrease during diagenesis. Ester bound components (fatty acids and alcohols) are also found to exponentially decrease during diagenesis (Glombitza et al., 2009a). Kinetic parameters of proton catalysed ester cleavage reactions have been also investigated by Glombitza et al. (2011) for the here studied New Zealand coal samples set.

374 Although the exact values of reaction rate constants (*k'*), activation energy (*Ea*), and
375 frequency factor (*A*) might be questionable due to experimental limitations, the general
376 trends of the ester cleavage reactions are still relevant. The *k'* values decrease with
377 increasing maturation indicating a slower cleavage reaction for more mature samples. Both
378 activation energies and frequency factors increase with maturation indicating that the
379 structure of kerogen has changed during maturation. The ester bonds within more mature
380 samples are sterically better protected due to a more compact structure of the organic
381 macromolecule. A higher activation energy and number of molecule collisions is needed
382 for the cleavage reactions to occur.

383 **4. Conclusions**

384 The structural evolution of organic matter in coals has been studied using a natural
385 maturity series from New Zealand. The study showed that the predominant structural
386 changes within the maturity range VR_r = 0.22 – 0.81% are related to oxygen loss during
387 degradation of functional groups. Using an empirical formula by Orr (1981) based on
388 pyrolysis yields and elemental composition it could be shown that oxygen loss directly
389 controls the increase in petroleum generating potential (i.e. HI values) of coals prior to
390 catagenesis. For the first time, the approximate amount of oxygen loss as CO_2 during
391 maturation of coals has been calculated from decreasing OI values during coalification.
392 This allows to quantify the feeding potential of any given coal type for deep biosphere
393 ecosystems. In case of the studied Late Cretaceous-Pleistocene coals, about 2.50E−4 to
394 1.25E−3 mg CO_2 are potentially generated from every litre of sediment per year. This rate
395 falls into the range of deep biosphere utilisation rates, and implies that coals, especially
396 immature ones, e.g. New Zealand coals, provide a large enough feeding potential for deep
397 microbial communities.

Acknowledgements

Financial support by the Vietnamese Overseas Scholarship Program (VOSP) in cooperation with the German Academic Exchange Service (DAAD), the Helmholtz Centre Potsdam and the New Zealand Foundation for Research, Science and Technology (contract C05X0302) is gratefully acknowledged. We thank F. Perssen (GFZ-Potsdam) and F. Leistner (Forschungszentrum Jülich) for their excellent technical support. We are grateful to Dr. Michael Erdmann and two anonymous reviewers for their suggestions and comments on scientific content, as well as their editorial efforts, which significantly improved the quality of the manuscript.

References

1. Al Sandouk-Lincke, N.A., Schwarzbauer, J., Volk, H., Hartkopf-Fröder, C., Fuentes, D., Young, M., Littke, R., 2013. Alteration of organic material during maturation: A pyrolytic and infrared spectroscopic study of isolated bisaccate pollen and total organic matter (Lower Jurassic, Hils Syncline, Germany). Organic Geochemistry 59, 22-36.

2. Avramidis, P., Zelilidis, A., 2007. Potential source rocks, organic geochemistry and thermal maturation in the southern depocenter (Kipourio-Grevena) of the Mesohellenic Basin, central Greece. International Journal of Coal Geology ICCP 2005 - Selected papers presented at the 57th Annual Meeting of the International Committee for Coal and Organic Petrology, Patras, Greece 71, 554-567.

3. Bechtel, A., Sachsenhofer, R.F., Zdravkov, A., Kostova, I., Gratzer, R., 2005. Influence of floral assemblage, facies and diagenesis on petrography and organic

geochemistry of the Eocene Bourgas coal and the Miocene Maritza-East lignite (Bulgaria). Organic Geochemistry 36, 1498-1522.

4. Behar, F., Vandenbroucke, M., Teermann, S.C., Hatcher, P.G., Leblond, C., Lerat, O., 1995. Experimental simulation of gas generation from coals and a marine kerogen. Chemical Geology Processes of Natural Gas Formation 126, 247-260.

5. Bertrand, P., 1984. Geochemical and petrographic characterization of humic coals considered as possible oil source rocks. Organic Geochemistry 6, 481-488.

6. Boreham, C.J., Horsfield, B., Schenk, H.J., 1999. Predicting the quantities of oil and gas generated from Australian Permian coals, Bowen Basin using pyrolytic methods. Marine and Petroleum Geology 16, 165-188.

7. Boudou, J.-P., Durand, B., Oudin, J.L., 1984. Diagenetic trends of a Tertiary low-rank coal series. Geochimica et Cosmochimica Acta 48, 2005-2010.

8. Carr, A.D., Williamson, J.E., 1990. The relationship between aromaticity, vitrinite reflectance and maceral composition of coals: Implications for the use of vitrinite reflectance as a maturation parameter. Advances in Organic Geochemistry 16, 313-323.

9. Charpenay, S., Serio, M.A., Bassilakis, R., Solomon, P.R., 1996. Influence of maturation on the pyrolysis products from coals and kerogens. a. Experiment. Energy & Fuels 10, 19-25.

10. D'Hondt, S., Rutherford, S., Spivack, A.J., 2002. Metabolic Activity of Subsurface Life in Deep-Sea Sediments. Science 295, 2067-2070.

441 11. Durand, B., Monin, J.C., 1980. Elemental analysis of kerogens (C, H, O, N, S, Fe).
442 in: Durand, B. (Ed.), Kerogen- insoluble organic matter from sedimentary rocks.
443 Technip, Paris, pp. 113-142.

444 12. Durand, B., Nicaise, G., Roucache, J., Vandenbroucke, M., Hagemann, H.W.,
445 1977. Etude géochimique d´une série de charbons. In: Campos, R., Goni, J. (Eds),
446 Advances in Organic Geochemistry 1975. Enadimsa, Madrid., 601-632.

447 13. Durand, B., Paratte, M., 1983. Oil potential of coals: A geochemical approach. In:
448 Brooks, J. (ed): Petroleum Geochemistry and Exploration of Europe. Gelogical
449 Society Special Publication, 255-265.

450 14. Espitalié, J., Deroo, G., Marquis, F., 1985. La pyrolise Rock- Eval et ses
451 applications. Revue de l'Institut Francais du Pétrole 40, 563-579.

452 15. Espitalié, J., Laporte, J.L., Madec, M., Marquis, F., Leplat, P., Paulet, J., Boutefeu,
453 A., 1977. Méthode rapide de caractérisation des roches mères de leur potentiel
454 pétrolier et de leur degré d´ évolution. Rev. Inst. Fr. Pét. 32, 23-42.

455 16. Fang, J., Zhang, L., 2011. Exploring the deep biosphere. Science China, Earth
456 Sciences 54, 157-165.

457 17. Glombitza, C., Mangelsdorf, K., Horsfield, B., 2009a. Maturation related changes
458 in the distribution of ester bound fatty acids and alcohols in a coal series from the
459 New Zealand Coal Band covering diagenetic to catagenetic coalification levels.
460 Organic Geochemistry 40, 1063-1073.

461 18. Glombitza, C., Mangelsdorf, K., Horsfield, B., 2009b. A novel procedure to detect
462 low molecular weight compounds released by alkaline ester cleavage from low

463 mature coals to assess its feedstock potential for deep microbial life. Organic
464 Geochemistry 40, 175-183.

465 19. Glombitza, C., Mangelsdorf, K., Horsfield, B., 2011. tructural insights from boron
466 tribromide ether cleavage into lignites and low maturity coals from the New
467 Zealand Coal Band. Organic Geochemistry 42, 228-236.

468 20. Hetényi, M., Sajgó, C., 1990. Hydrocarbon generation potential of some Hungarian
469 low-rank coals. Organic Geochemistry 16, 907-916.

470 21. Horsfield, B., Kieft, T.L., Group, t.G., 2007. The GeoBiosphere, in: Harms, U.,
471 Koeberl, C., Zoback, M.D. (Eds.), Continental Scientific Drilling- A decade of
472 progress, and challenges for the future. Springer, Berlin, ISBN-10: 3642088309,
473 pp. 163-211.

474 22. Horsfield, B., Schenk, H.J., Zink, K., Ondrak, R., Dieckmann, V., Kallmeyer, J.,
475 Mangelsdorf, K., Primio, R.d., Wilkes, H., Parkes, R.J., Fry, J., Cragg, B., 2006.
476 Living microbial ecosystems within the active zone of catagenesis: Implications for
477 feeding the deep biosphere. Earth and Planetary Science Letters 246, 55-69.

478 23. Hvoslef, S., Larter, S.R., Leythaeuser, D., 1988. Aspects of generation and
479 migration of hydrocarbons from coal-bearing strata of the Hitra Formation,
480 Haltenbanken area, offshore Norway. Organic Geochemistry 13, 525-536.

481 24. Ibarra, J., Muñoz, E., Moliner, R., 1996. FTIR study of the evolution of coal
482 structure during the coalification process. Organic Geochemistry 24, 725-735.

483 25. Jasper, K., Kross, B.M., Flajs, G., Hartkopf-Fröder, C., Littke, R., 2009.
484 Characteristics of type III kerogen in coal-bearing strata from the Pennsylvanian

(Upper Carboniferous) in the Ruhr Basin, Western Germany: Comparison of coals, dispersed organic matter, kerogen concentrates and coal–mineral mixtures. Internaltional Journal of Coal Geology 80, 1-19.

26. Kelemen, S.R., Afeworki, M., Gorbaty, M.L., 2002. Characterization of organically bound oxygen forms in lignites, peats, and pyrolyzed peats by X-ray photoelectron spectroscopy (XPS) and solid-state 13C NMR methods. Energy & Fuels 16, 1450-1462.

27. Kelemen, S.R., Afeworki, M., Gorbaty, M.L., Sansone, M., Kwiatek, P.J., Walters, C.C., Freund, H., Siskin, M., 2007. Direct characterization of kerogen by X-ray and solid-state 13C nuclear magnetic resonance methods. Energy & Fuels 21.

28. Kelemen, S.R., Kwiatek, P.J., 1995. Quantification of organic oxygen species on the surface of fresh and reacted Argonne premium coal. Energy & Fuels 9, 841-848.

29. Kelemen, S.R., Rose, K.D., Kwiatek, P.J., 1993. Carbon aromaticity based on XPS II to II□ signal intensity. Applied Surface Science 64, 167-174.

30. Killops, S.D., Allis, R.G., Funnel, R.H., 1996. Carbon dioxide generation from coals in Taranaki Basin, New Zealand: Implications for petroleum migration in Southeast Asian Tertiary basins. AAPG Bulletin 80, 545-569.

31. Killops, S.D., Funnell, R.H., Suggate, R.P., Sykes, R., Peters, K.E., Walters, C., Woolhouse, A.D., Weston, R.J., Boudou, J.-P., 1998. Predicting generation and expulsion of paraffinic oil from vitrinite-rich coals. Organic Geochemistry 29, 1-21.

32. Killops, S.D., Woolhouse, A.D., Weston, R.J., Cook, A.R., 1994. A geochemical appraisal of oil generation in the Taranaki basin, New Zealand. American Association of Petroleum Geologists Bulletin 78, 1560-1585.

33. Krumholz, L.R., McKinley, J.P., Ulrich, G.A., Suflita, J.M., 1997. Confined subsurface microbial communities in Cretaceous rock. Nature 386, 64-66.

34. L'Haridon, S., Reysenbacht, A.L., Glenat, P., Prieur, D., Jeanthon, C., 1995. Hot subterranean biosphere in a continental oil reservoir. Nature 377, 223-224.

35. Landais, P., 1991. Assessment of coal potential evolution by experimental simulation of natural coalification. Organic Geochemistry 17, 705-710.

36. Levine, J.R., 1993. Coalification: The evolution of coal as source rock and reservoir rock for oil and gas. In: Law, B.E., Dudley, D.R. (Eds.), Hydrocarbons from coal. AAPG Studies in Geology 38, 39-77.

37. Mahlstedt, N., Horsfield, B., 2012. Metagenetic methane generation in gas shales I. Screening protocols using immature samples. Marine and Petroleum Geology 31, 27-42.

38. Marchand, A., Conard, J., 1980. Electron paramagnetic reso- nance in kerogen studies, in: Durand, B. (Ed.), Kerogen, Insoluble Organic Matter from Sedimentary Rocks. Technip, Paris, pp. 243-270.

39. Marquis, F., Lafargue, E., Espitalié, J., 1992. The influence of maceral composition and maturity on the petroleum-generating potential of coals, in A.M. Spencer, ed., Generation, accumulation, and production of Europe´s hydrocarbons II: New York,

528 Springer-Verlag, Special Publication of the European Association of Petroleum
529 Geoscientists. 239-247.

530 40. Newman, J., Price, L.C., Johnston, J.H., 1997. Hydrocarbon source potential and
531 maturation in Eocene New Zealand vitrinite-rich coals: insights from traditional
532 coal analysis, and Rock-Eval and biomarker studies. Journal of Petroleum Geology
533 20, 137-163.

534 41. Norgate, C.M., Boreham, C.J., Kamp, P.J.J., Newman, J., 1997. Relationships
535 between hydrocarbon generation, coal type and rank for Middle Eocene coals,
536 Buller Coalfield, New Zealand. Journal of Petroleum Geology 20, 427-458.

537 42. Oberlin, A., Boulmier, J.L., Villey, M., 1980. Electron micro- scopic study of
538 kerogen microtexture. Selected criteria for determining the evolution path and
539 evolution stage of kerogen., in: Durand, B. (Ed.), Kerogen, Insoluble Organic
540 Matter from Sedimentary Rocks. Technip, Paris, pp. 191-241.

541 43. Orr, W.L., 1981. Comments on pyrolytic hydrocarbon yields in source-rock
542 evaluation. Advances in Organic Geochemistry 1981 (Eds. Bjoroy M.), 775-787.

543 44. Parkes, R.J., Cragg, B.A., Wellsbury, P., 2000. Recent studies on bacterial
544 polulations and processes in subseefloor sediments: A review. Hydrogeology
545 Journal 8, 11-28.

546 45. Payne, D.F., Ortoleva, P.J., 2001. A model for lignin alteration-part I: a kinetic
547 reaction-network model. Organic Geochemistry 32, 1073-1085.

548 46. Pelet, R., 1985. Évaluation quantitative des produits formés lors de l´ évolution
549 géochimique de la matière organicque. Revue de I´Institut Français du Pétrole 40,
550 551-562.

551 47. Requejo, A.G., Gray, N.R., Freund, H., 1992. Maturation of petroleum source
552 rocks. 1. Changes in kerogen structure and composition associatedwith
553 hydrocarbon generation. . Energy & Fuels 6, 203-214.

554 48. Rice, D.D., Claypool, G.E., 1981. Generation, accumulation, and resource potential
555 of biogenic gas. AAPG Bulletin 65, 5-25.

556 49. Robin, P.L., Rouxhet, P.G., 1978. Characterization of kerogens and study of their
557 evolution by infrared spectroscopy: carbonyl and carboxyl groups. Geochimica et
558 Cosmochimica Acta 42, 1341-1349.

559 50. Salmon, E., Behar, F., Lorant, F., Hatcher, P.G., Marquaire, P.-M., 2009. Early
560 maturation processes in coal. Part 1: Pyrolysis mass balance and structural
561 evolution of coalified wood from the Morwell Brown Coal seam. Organic
562 Geochemistry 40, 500-509.

563 51. Schenk, H.J., Horsfield, B., 1998. Using natural maturation series to evaluate the
564 utility of parallel reaction kinetics models: an investigation of Toarcian shales and
565 Carboniferous coals, Germany. Organic Geochemistry 29, 137-154.

566 52. Schenk, H.J., Richter, A., 1995. Investigation of carboniferous coals by infrared
567 spectroscopy and kinetic measurements. Unpublished data.

568 53. Schenk, H.J., Witte, E.G., Muller, P.J., Schwochau, K., 1986. Infrared estimates of
569 aliphatic kerogen carbon in sedimentary rocks. Organic Geochemistry 10, 1099-
570 1104.

571 54. Solomon, P.R., Hamblen, D.G., Carangelo, R.M., Serio, M.A., Deshpande, G.V.,
572 1988. General model for coal devolatilization. Energy & Fuels 2, 405-422.

573 55. Stach, E., Mackowsky, M.-T., Teichmüller, M., Taylor, G.H., Chandra, D.,
574 Teichmüller, R., 1982. Stach´s textbook of coal petrology.

575 56. Suggate, R.P., 1959. New Zealand coals: their geological setting and its influence
576 on their properties. New Zealand Department of Scientific and Industrial Research
577 Bulletin 134.

578 57. Suggate, R.P., 2000. The Rank(Sr) scale: its basis and its applicability as a maturity
579 index for all coals. New Zealand Journal of Geology and Geophysics 43, 521-553.

580 58. Suggate, R.P., 2002. Application of Rank (Sr), a maturity index based on chemical
581 analyses of coals. Marine and Petroleum Geology 19, 929-950.

582 59. Suggate, R.P., Boudou, J.-P., 1993. Coal rank and type variation in Rock-Eval
583 assessment of New Zealand coals. Journal of Petroleum Geology 16, 73-88.

584 60. Sykes, R., 2004. Peat biomass and early diagenetic controls on the paraffinic oil
585 potential of humic coals, Canterbury Basin, New Zealand. Petroleum Geoscience
586 10, 283-303.

587 61. Sykes, R., Snowdon, L.R., 2002. Guidelines for assessing the petroleum potential
588 of coaly source rocks using Rock-Eval pyrolysis. Organic Geochemistry 33, 1441-
589 1455.

590 62. Sykes, R., Snowdon, L.R., Johansen, P.E., 2004. Leaf biomass-a new paradigm for
591 sourcing the terrestrial oils of Taranaki Basin. In: Boult, P.J.; Johns, D.R. & Lang,
592 S.C. (Eds), Eastern Australasian Basin Symposium II. Petroleum Exploration
593 Society of Australia, Special Publication, 553-574.

594 63. Sykes, R., Suggate, R.P., King, P.R., 1992. Timing and depth of maturation in
595 southern Taranaki Basin from reflectance and Rank(Sr). 1991 New Zealand Oil
596 Exploration Conference Proceedings,373-389. Crown Minerals, Ministry of
597 Commerce, Wellington.

598 64. Taylor, G.H., Teichmüller, M., Davis, A., Diessel, C.F.K., Littke, R., Rorbert, P.,
599 1998. Organic petrology. Gebruder Borntraeger, Berlin-Stuttgart, 704p.

600 65. Tissot, B., Durand, B., Espitalie´, J., Combaz, A., 1974. Influence of Nature and
601 Diagenesis of Organic Matter in formation of Petroleum. AAPG Bulletin 58, 499-
602 506.

603 66. Tissot, B.P., Welte, D.H., 1984. Petroleum Formation and Occurrence. Springer-
604 Verlag Berlin Heidelberg New York Tokyo.

605 67. Vandenbroucke, M., Largeau, C., 2007. Kerogen origin, evolution and structure.
606 Organic Geochemistry 38, 719-833.

607 68. Vieth, A., Mangelsdorf, K., Sykes, R., Horsfield, B., 2008. Water extraction of
608 coals – potential for estimating low molecular weight organic acids as carbon
609 feedstock for the deep terrestrial biosphere. Organic Geochemistry 39, 1606-1619.

610 69. Vu, T.A.T., 2008. Origin and maturation of organic matter in New Zealand coals.
611 Ph.D Thesis, University of Greifswald, 268p.

612 70. Vu, T.A.T., Horsfield, B., Sykes, R., 2008. Influence of in-situ bitumen on the
613 generation of gas and oil in New Zealand coals. Organic Geochemistry 39, 1606-
614 1619.

615 71. Vu, T.A.T., Zink, K.G., Mangelsdorf, K., Sykes, R., Wilkes, H., Horsfield, B.,
616 2009. Changes in bulk properties and molecular compositions within New Zealand
617 Coal Band solvent extracts from early diagenetic to catagenetic maturity levels. .
618 Organic Geochemistry 40, 963-977.

619 72. Witte, E.G., Schenk, H.J., Müller, P.J., Schwochau, K., 1988. Structural
620 modifications of kerogen during natural evolution as derived from 13C CP/MAS
621 NMR, IR spectroscopy and Rock-Eval pyrolysis of Toarcian shales. Proceedings of
622 the 13th International Meeting on Organic Geochemistry 13, 1039-1044.

Figure and Table captions

Figure 1: Plot of volatile matter (in percent) against calorific value (in British thermal units per pound) for the investigated coals showing their positions in the New Zealand Coal Band and the Rank(S_r) scale of Suggate (2000). Volatile matter and calorific values are on the dry, mineral matter and sulphur free (dmmsf) basis.

Figure 2: The loss of oxygen during maturation of New Zealand coals representing as the decreases of (a) O/C atomic ratios, (b) the absolute contents of oxygen on dried ash free basic (daf, %), (c) the moisture contents, (d) the Oxygen Index, (e) the total organic oxygen (amount per 100C), and (f) the infrared C=O adsorption as function of vitrinite reflectance.

Figure 3: The XPS results for carbon−oxygen single and multiply bonded species plotted as a function of the vitrinite reflectance.

Figure 4: The measured HI values revealed from Rock-Eval analysis of the samples in Group A, New Zealand coal (a) as a function of maturation, (b) in comparison with the calculated HI values from the elemental atomic O/C and H/C ratios, and (c, d) in the direct correlations with the elemental atomic H/C and O/C ratios.

Figure 5: The evolution of organic matter structures as revealed from (a) Rock-Eval pyrolysis, (b, c) infrared spectroscopy, (d) X-ray photoelectron spectroscopy and (e–h) pyrolysis gas chromatography in course of maturation (vitrinite reflectance) for the New Zealand coals. HI = Hydrogen Index, Aro-CH = aromatic CH, ali-(CH_2+CH_3) = aliphatic CH_2 plus CH_3, aro-C = total aromatic carbon, ali-C = total aliphatic carbon, C_{6+} = bulk C_{6+} pyrolysis yield, phenols = sum of phenol and cresols, *n*C_{6+} = resolved C_{6+} pyrolysis yield, MA = sum of monoaromatics, DA = sum of diaromatics, GOR = C_{1-5}/ C_{6+}.

Figure 6: The Transformation Ratio of CO_2 as a function of vitrinite reflectance (a) and against the yields of CO_2 released during maturation (b).

Tables

Table 1: List of studied samples indicating maturity parameter (VR_r), bulk geochemical parameters (TOC, Moisture, Oxygen contents), Rock-Eval parameters (S1, S2, S3, HI, OI), elemental compositions (O/C, H/C), calculated HI values from the elemental compositions, gas wetness (%) and aromaticity. VR_r = vitrinite reflectance; TOC = total organic carbon; Oxygen = absolute oxygen contents on dried ash free basic (daf, %); HI = Hydrogen Index; OI = Oxygen Index; wetness = C_{1-5}/ C_{2-5}, aromaticity = aromatic moieties/*n*-alkyl moieties in C_{6+}; *n.d* = not detected.

Table 2: Integrated infrared absorptions (cm/mg TOC) in selected spectral ranges of selected New Zealand coals. VR_r = vitrinite reflectance, K 300-2700 = C-H stretching vibrations of aliphatic CH_2 and CH_3 groups, K 1520-1340 = asymmetric bending vibrations of aliphatic CH_2 and CH_3 groups, K 1390-1340 = asymmetric bending vibrations of aliphatic CH_3 group, K 900-700 = out-of-plane vibrations of aromatic CH groups, K-1700 = infrared C=O adsorption, *n.d* = not detected.

Table 3: XPS results consisting amounts of aromatic carbon, calculated aliphatic carbon, total organic oxygen, and forms of organic oxygen.

Table 4: List of studied samples indicating maturity parameter (VR_r), measured Oxygen Index (OI) from Rock-Eval analysis, calculated Transformation Ratio of CO_2 (TR_{CO2}), Oxygen Index normalised to the original organic carbon content of the original sample, and the released CO_2 yields.

49 Table 5: Calculated feedstock potential of the investigated New Zealand coals as compared
50 with rates of deep biosphere respiration. * CO_2 respiration rates from D'Hondt et al.
51 (2002)

52

HIGHLIGHTS

- Structural evolution of coals during diagenesis to moderate catagenesis was studied
- Structural changes are related to oxygen loss during defunctionalisation processes
- Oxygen loss directly causes an increase in petroleum generating potential of coals
- CO2 generation rate (2.5E-4 to 1.25E-3 mg/l/a) was calculated from the drop of OI
- It allows quantifying feeding potential for deep biosphere of any given coal types

Sample	Group	VR_r	TOC	Moisture	Oxygen	S1	S2	S3	HI	OI	O/C	H/C
		%	%	%	%, daf	mg/g sediment			mg/g TOC		atomic ratios	
G001985	Group A	0,25	48,5	15,5	*n.d*	22,4	75,5	46,0	156	95	*n.d*	*n.d*
G001988		0,27	48,6	15,7	29,9	19,6	64,8	43,5	133	89	0,343	0,901
G001979		0,25	48,9	38,4	29,5	13,8	72,6	52,3	148	107	0,338	0,868
G001987		0,26	46,9	28,5	29,1	13,0	58,0	45,4	124	97	0,328	0,855
G001986		0,27	49,9	22,5	28,4	18,7	70,3	41,4	141	83	0,318	0,863
G001976		0,29	54,4	15,9	27,3	16,4	82,6	44,5	152	82	0,304	0,838
G001978		0,28	53,7	24,1	26,0	7,5	69,3	39,4	129	73	0,281	0,820
G001975		0,29	51,6	17,3	27,0	9,8	69,6	39,5	135	77	0,292	0,860
G001983		0,41	58,5	16,7	22,3	7,3	94,0	28,4	161	49	0,230	0,809
G001977		0,39	59,5	17,0	22,1	6,2	101,3	21,4	170	36	0,227	0,784
G001982		0,40	60,0	17,8	21,3	4,0	105,2	23,3	175	39	0,218	0,811
G001984		0,45	63,9	10,6	20,1	3,7	108,5	17,0	170	27	0,202	0,803
G001981		0,45	61,2	15,1	20,6	3,0	94,5	19,9	154	32	0,208	0,778
G001992		0,49	64,9	12,7	*n.d*	4,5	113,9	20,5	176	32	*n.d*	*n.d*
G001980		0,44	60,2	11,0	18,8	3,0	104,0	15,5	173	26	0,179	0,795
G001995		0,52	68,3	10,5	17,5	3,2	134,9	10,6	198	16	0,172	0,782
G001997		0,52	67,4	8,8	17,7	2,9	141,1	9,9	209	15	0,174	0,817
G001996		0,52	65,5	5,9	15,4	4,0	150,5	8,4	230	13	0,143	0,829
G001994		0,61	63,5	7,0	*n.d*	6,2	179,9	9,1	283	14	0,120	0,843
G001993		0,76	77,8	3,3	10,5	6,9	193,3	3,9	248	5	0,095	0,779
G001990		0,71	74,2	2,9	11,2	7,6	198,3	4,3	267	6	0,098	0,802
G001989		0,69	73,3	3,3	11,7	10,9	190,8	2,4	260	3	0,111	0,807
G001991		0,80	75,0	2,3	*n.d*	13,7	194,0	3,7	259	5	0,068	0,823
G002610	Group B	0,22	59,7	38,3	24,8	3,7	106,4	16,9	178	28	0,264	0,841
G002600		0,30	57,9	39,4	24,3	3,0	92,4	19,8	160	34	0,258	0,883
G002570		0,33	63,4	27,3	18,1	3,4	120,1	16,0	189	25	0,177	0,845
G002590		0,50	70,5	14,1	16,0	2,7	93,2	14,2	132	20	0,153	0,789
G002587		0,68	78,0	5,0	11,1	6,0	99,1	21,3	127	27	0,102	0,808
G002585		0,81	74,5	4,0	11,5	3,0	189,0	1,6	254	2	0,102	0,798

HI	Wetness	Aromaticity
calculated	%	
n.d	52	0,20
150	50	0,22
131	48	0,27
130	50	0,25
144	49	0,21
137	48	0,29
143	44	0,30
162	45	0,29
176	49	0,32
162	48	0,30
188	49	0,26
194	49	0,29
172	47	0,27
n.d	48	0,26
207	48	0,27
203	50	0,27
226	50	0,24
260	49	0,24
287	53	0,13
264	49	0,25
276	49	0,18
270	52	0,24
315	50	0,23
n.d	*n.d*	*n.d*
n.d	*n.d*	*n.d*
n.d	*n.d*	*n.d*
n.d	*n.d*	*n.d*
n.d	*n.d*	*n.d*
n.d	*n.d*	*n.d*

Sample	VR_r	K 3000-2700	K 1520- 1390	K 1390- 1340	K 900- 700	K-1700
	%	cm/mg TOC				
G001988	0,27	26,08	*n.d.*	*n.d.*	*n.d.*	45,95
G001986	0,27	21,78	*n.d.*	*n.d.*	*n.d.*	55,16
G001977	0,39	24,08	6,54	1,63	5,69	36,95
G001984	0,45	22,32	7,44	1,35	18,26	49,21
G001981	0,45	18,21	6,22	1,59	3,99	43,84
G001980	0,44	19,88	6,73	1,38	3,68	42,68
G001995	0,52	22,80	10,86	1,30	7,76	40,83
G001997	0,52	21,62	9,25	1,12	5,82	39,57
G001996	0,52	21,98	9,51	0,82	4,21	42,65
G001991	0,80	31,80	14,62	0,78	10,85	16,07
G002610	0,22	19,02	*n.d.*	*n.d.*	*n.d.*	43,14
G002600	0,30	14,04	*n.d.*	*n.d.*	*n.d.*	34,00
G002570	0,33	15,59	3,69	0,78	4,22	34,56
G002590	0,50	19,03	7,30	1,03	6,46	32,24
G002587	0,68	23,49	12,09	0,87	10,85	19,53
G002585	0,81	23,89	11,61	0,57	5,68	26,09

Sample	VR_r	Aromatic C	Aliphatic C	Total organic Oxygen	C-O	C=O
					286.3eV	287.5eV
	%	a mount per 100 C		a mount per 100 C		a mount per 100
G001988	0,27	39,0	41,5	15,9	6,7	3,2
G001986	0,27	38,0	32,4	20,9	11,7	3,4
G001977	0,39	47,0	34,7	14,9	6,2	3,3
G001984	0,45	53,0	27,0	14,3	7,6	3,1
G001981	0,45	56,0	19,7	17,9	8,8	4,5
G001980	0,44	55,0	27,1	13,4	7,0	1,4
G001995	0,52	61,0	23,2	10,4	6,6	1,4
G001997	0,52	68,0	14,6	12,9	6,7	1,8
G001996	0,52	61,0	24,1	9,4	6,7	0,3
G001991	0,80	70,0	18,0	6,5	5,5	1,0
G002610	0,22	47,0	30,7	18,9	7,6	2,9
G002600	0,30	46,0	34,1	15,1	7,7	1,6
G002570	0,33	54,0	28,3	13,3	6,9	1,6
G002590	0,50	68,0	12,4	12,9	7,9	2,8
G002587	0,68	63,0	23,5	7,7	6,5	0,0
G002585	0,81	73,0	14,1	6,8	6,4	0,0

O-C=O 289.0eV	**C-O**	**C=O**	**O-C=O**
C		%	
6,0	42,0	20,2	37,9
5,8	55,9	16,3	27,8
5,4	41,4	22,2	36,4
3,6	53,0	21,8	25,3
4,6	49,0	25,2	25,8
5,0	52,2	10,4	37,3
2,4	63,5	13,5	23,1
4,4	51,9	14,0	34,1
2,4	71,3	3,2	25,5
0,0	84,6	15,4	0,0
8,4	40,2	15,3	44,4
5,8	51,0	10,6	38,4
4,8	51,7	12,1	36,2
2,2	61,1	21,8	17,1
1,2	84,3	0,0	15,7
0,4	94,1	0,0	5,9

Sample	VR_r	OI	TR_{CO2}	Normalised OI	CO_2 yield
	%	(mg /g TOC)	%	mg/g TOC	mg/g TOC
G001979	0,25	106,79	0,00	106,8	0,0
G001987	0,26	96,98	0,09	96,7	10,1
G001985	0,25	94,79	0,12	94,5	12,3
G001988	0,27	89,43	0,17	89,0	17,8
G001986	0,27	82,89	0,23	82,3	24,5
G001976	0,29	81,72	0,24	81,1	25,6
G001975	0,29	76,58	0,29	75,9	30,9
G001978	0,28	73,37	0,32	72,7	34,1
G001983	0,41	48,60	0,55	47,8	59,0
G001982	0,40	38,88	0,64	38,1	68,7
G001977	0,39	35,96	0,67	35,2	71,5
G001981	0,45	32,44	0,70	31,8	75,0
G001992	0,49	31,55	0,71	30,9	75,9
G001984	0,45	26,56	0,76	26,0	80,8
G001980	0,44	25,78	0,76	25,2	81,6
G001995	0,52	15,54	0,86	15,1	91,6
G001997	0,52	14,75	0,87	14,4	92,4
G001994	0,61	14,32	0,87	14,0	92,8
G001996	0,52	12,82	0,88	12,5	94,3
G001990	0,71	5,73	0,95	5,6	101,2
G001993	0,76	5,02	0,95	4,9	101,9
G001991	0,80	4,91	0,96	4,8	102,0
G001989	0,69	3,21	0,97	3,1	103,7

CO_2 respiration rates*	Minimum	Maximum
mmol/l/a	1,00E-06	1,00E-03
mg/l/a	4,40E-05	4,40E-02
CO_2 generation	**Minimum**	**Maximum-Late Cretaceous**
mg/g TOC	10	100
mmol/g TOC	0,23	2,4
Timeframe in Ma	2	100
Average density of sediment		
kg/l	2	2
Feedstock	**Maximum**	**Minimum**
mg/kg sediment/a	2,50E-03	5,00E-04
mg/l sediment/a	1,25E-03	2,50E-04

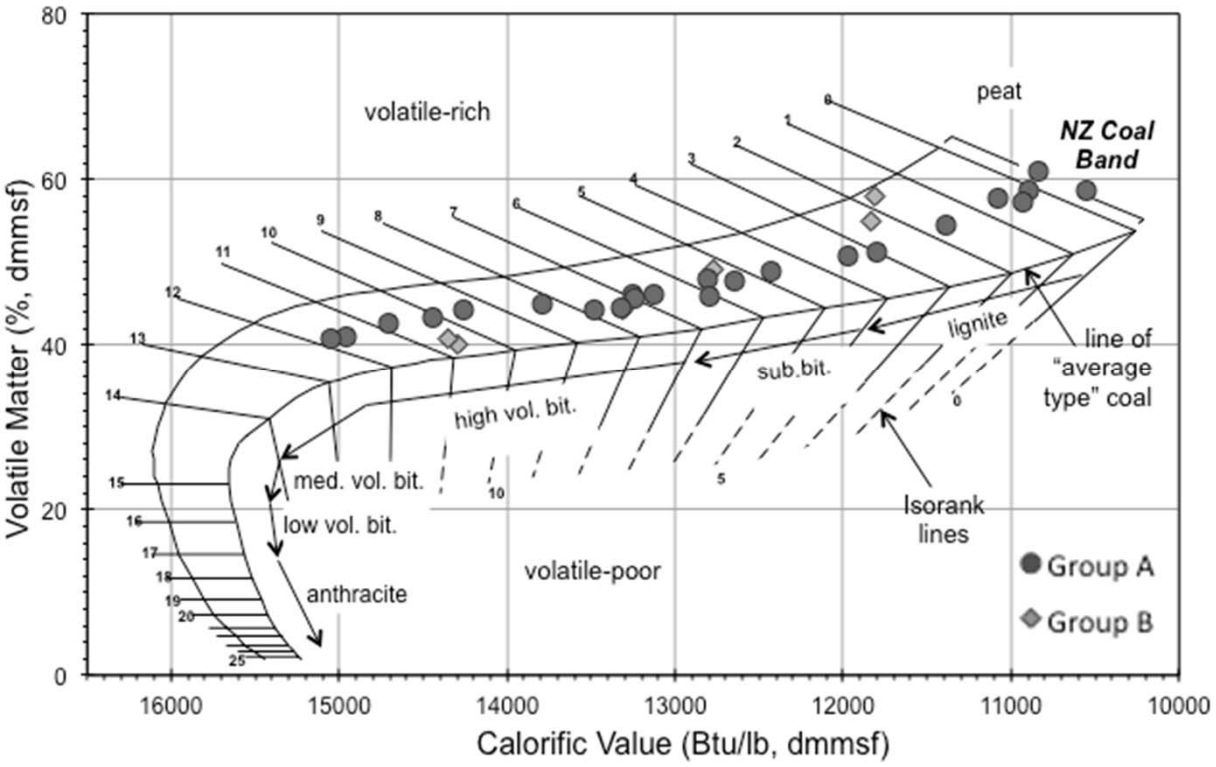
Volatile Matter (%, dmmsf)
Calorific Value (Btu/lb, dmmsf)
volatile-rich
volatile-poor
peat
NZ Coal Band
lignite
sub.bit.
high vol. bit.
med. vol. bit.
low vol. bit.
anthracite
line of "average type" coal
Isorank lines
Group A
Group B

Fig. 1

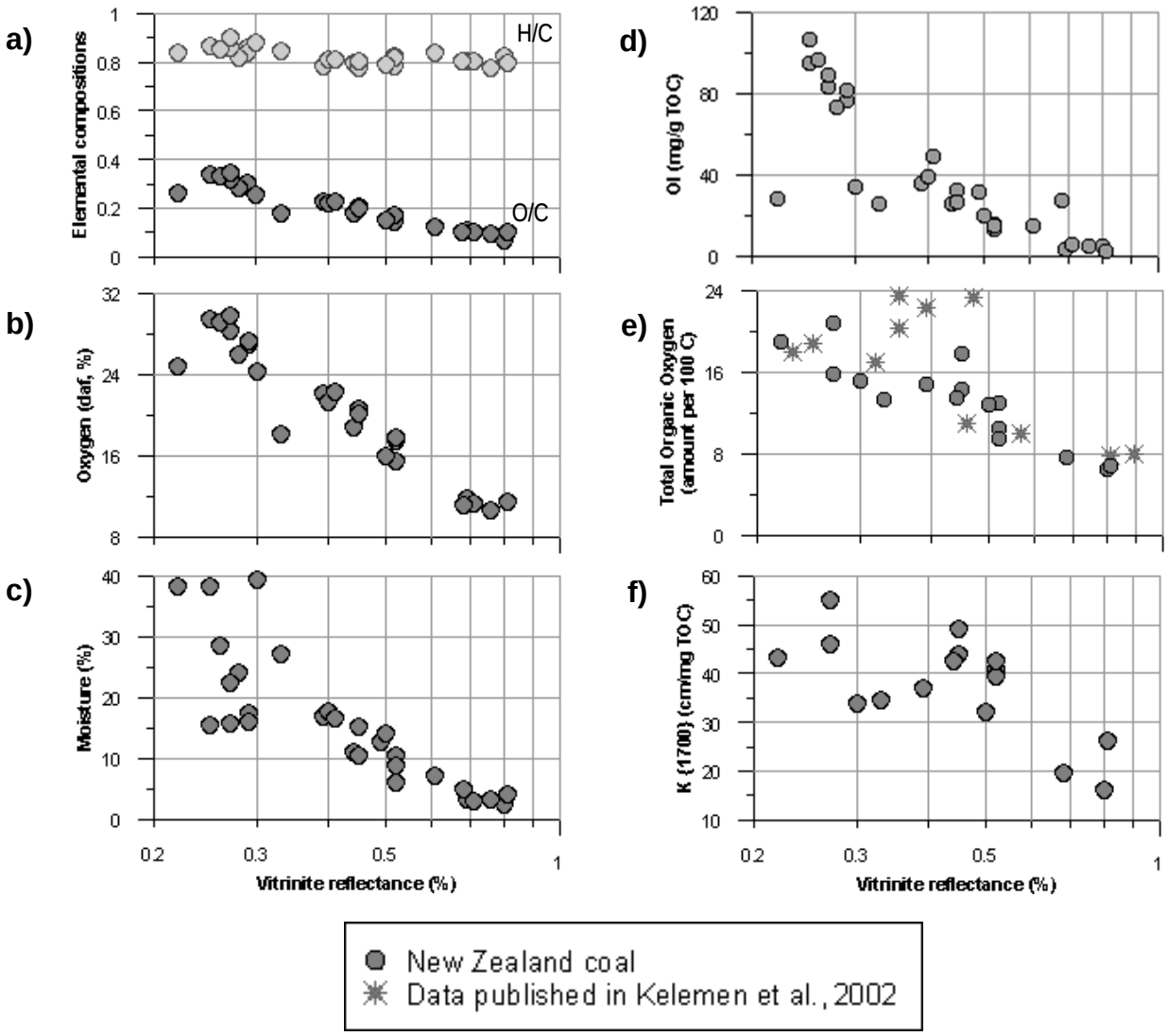
a)
b)
c)
d)
e)
f)
Elemental compositions
H/C
O/C
Oxygen (daf, %)
Moisture (%)
OI (mg/g TOC)
Total Organic Oxygen (amount per 100 C)
K (1700) (cm/mg TOC)
Vitrinite reflectance (%)
Vitrinite reflectance (%)
New Zealand coal
Data published in Kelemen et al., 2002

Fig. 2

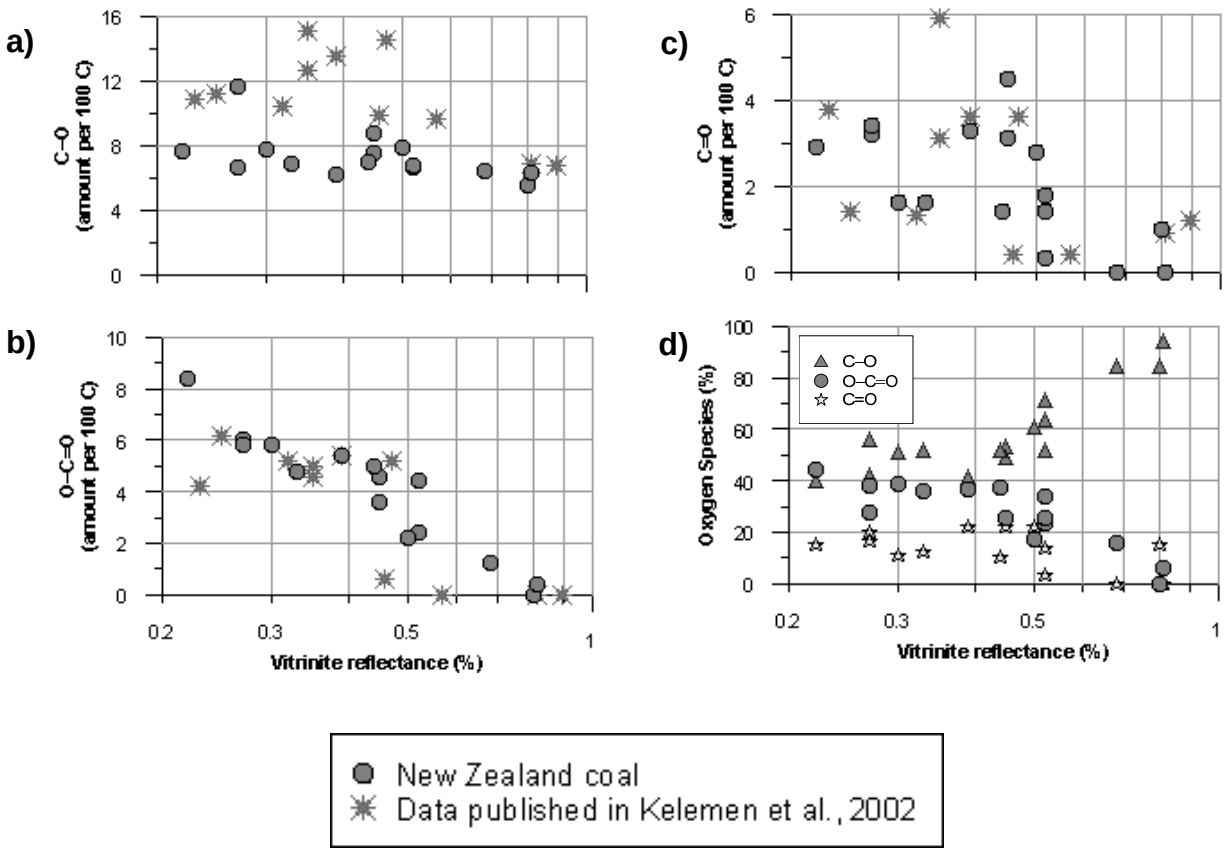

New Zealand coal
Data published in Kelemen et al., 2002

Fig. 3

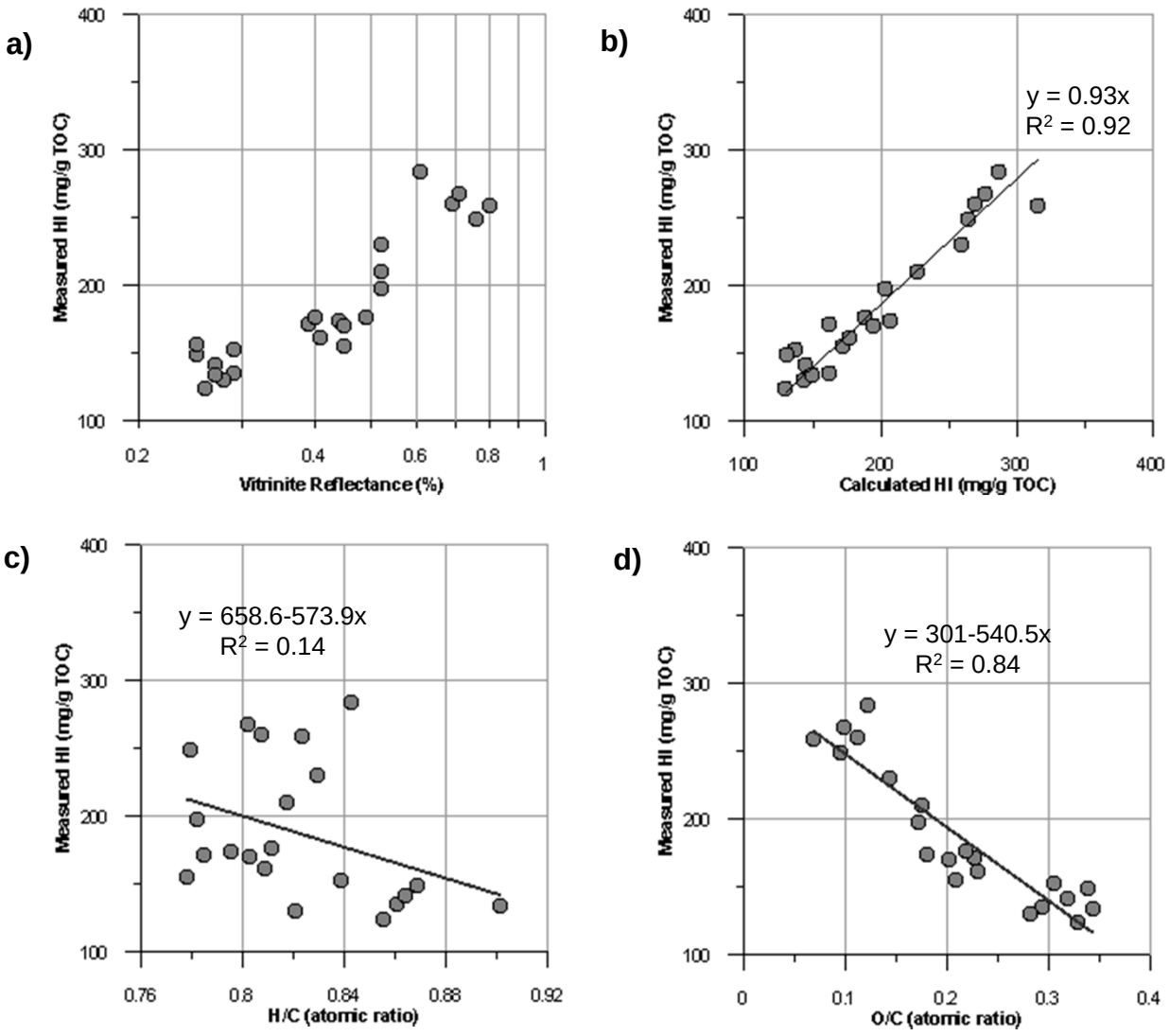
a)
Measured HI (mg/g TOC)
400
300
200
100
0.2
0.4
0.6
0.8
1
Vitrinite Reflectance (%)
b)
Measured HI (mg/g TOC)
y = 0.93x
R2 = 0.92
100
200
300
400
Calculated HI (mg/g TOC)
c)
Measured HI (mg/g TOC)
y = 658.6-573.9x
R2 = 0.14
0.76
0.8
0.84
0.88
0.92
H/C (atomic ratio)
d)
Measured HI (mg/g TOC)
y = 301-540.5x
R2 = 0.84
0
0.1
0.2
0.3
0.4
O/C (atomic ratio)

Fig. 4

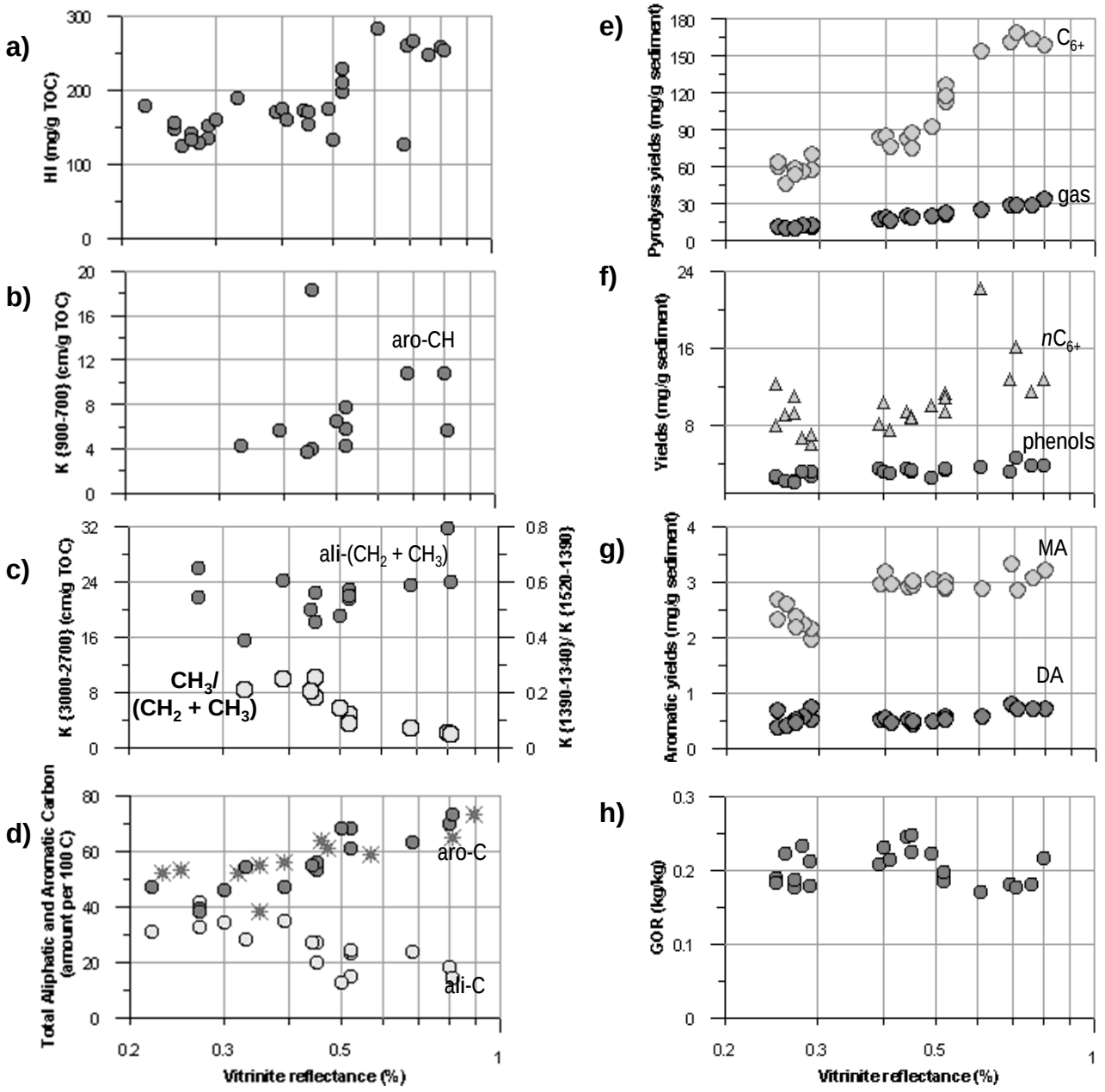
a)
HI (mg/g TOC)
b)
K {900-700} (cm/g TOC)
aro-CH
c)
K {3000-2700} (cm/g TOC)
ali-(CH2 + CH3)
CH3/
(CH2 + CH3)
K {1390-1340}/ K {1520-1390}
d)
Total Aliphatic and Aromatic Carbon (amount per 100 C)
aro-C
ali-C
Vitrinite reflectance (%)
e)
Pyrolysis yields (mg/g sediment)
C6+
gas
f)
Yields (mg/g sediment)
nC6+
phenols
g)
Aromatic yields (mg/g sediment)
MA
DA
h)
GOR (kg/kg)
Vitrinite reflectance (%)

Fig. 5

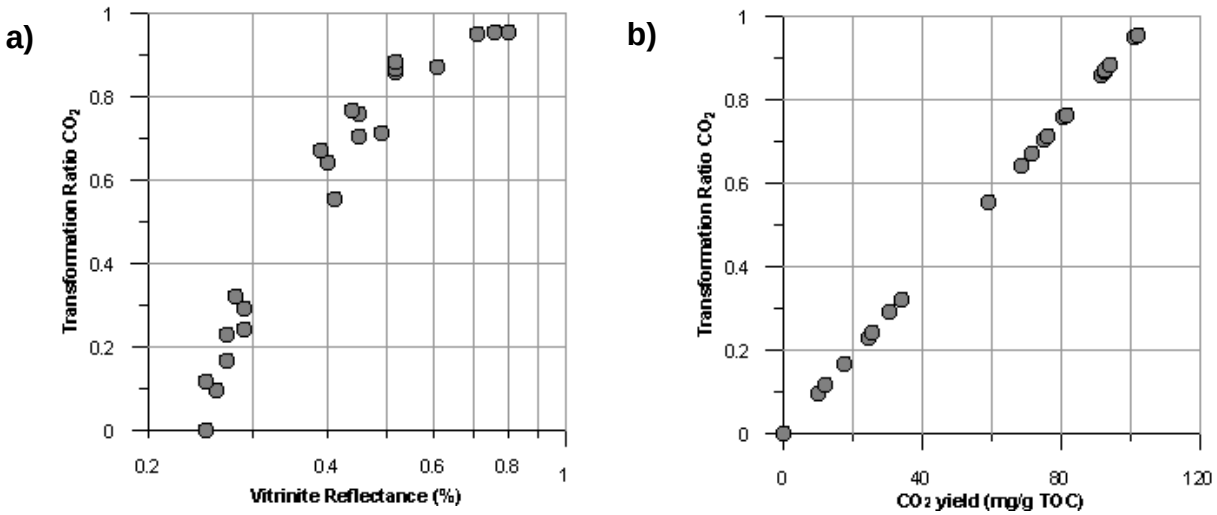
a)
Transformation Ratio CO_2
Vitrinite Reflectance (%)
0
0.2
0.4
0.6
0.8
1
b)
Transformation Ratio CO_2
CO_2 yield (mg/g TOC)
0
40
80
120

Fig. 6